Macromolecules

Article

pubs.acs.org/Macromolecules

Conjugated Polymer Consisting of Quinacridone and Benzothiadiazole as Donor Materials for Organic Photovoltaics: Coplanar Property of Polymer Backbone

Ho-Jun Song,[†] Doo-Hun Kim,[†] Eui-Jin Lee,[†] Soo-Won Heo,[†] Jang-Yong Lee,[‡] and Doo-Kyung Moon[†,*]

[†]Department of Material Chemistry and Engineering, Konkuk University, Seoul, 143-701, Republic of Korea

[‡]Energy Materials Research Center, Korea Research Institute of Chemical Technology, P.O. Box 107, Yuseong, Daejeon 305-600, Republic of Korea

Supporting Information

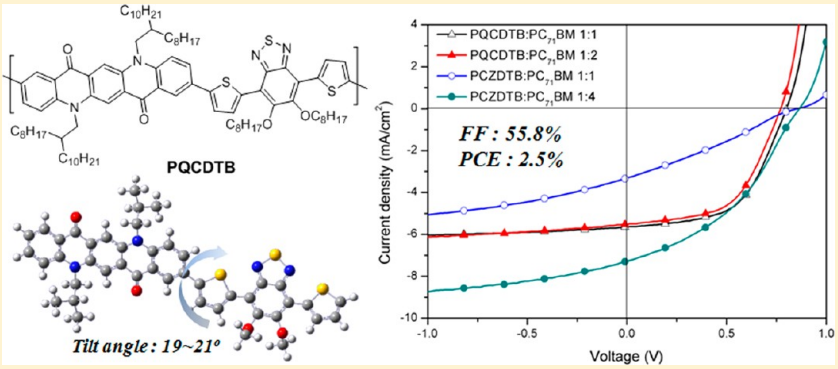

ABSTRACT: Highly soluble poly[quinacridone-*alt*-benzothiadiazole] (PQCDTB) has been synthesized through the Suzuki coupling reaction by introducing planar quinacridone and highly absorbing benzothiadiazole. The PQCDTB dissolved in general organic solvents, and the M_n was 49.8 kg/mol. The optical band gap energy was 1.92 eV, which was similar to the band gap of benzothiadiazole. The HOMO and LUMO levels of PQCDTB were −5.24 eV and −3.32 eV, respectively. According to the XRD measurement, PQCDTB showed the formation of ordered lamellar structure as an out-of-plane peak (*h*00) by the alkyl side chain of quinacridone and conventional edge-on π- stacking. This study also evaluated the OPV characteristics by fabricating a bulk-heterojunction−type polymer solar cell. When PQCDTB and $PC_{71}BM$ were fabricated in a 1:1 weight ratio, the open-circuit voltage (V_{OC}), short-circuit current (J_{SC}), fill factor (FF), and power conversion efficiency (PCE) were 0.79 V, 5.6 mA cm^{-2}, 55.8% and 2.5%, respectively. In particular, PQCDTB exhibited higher FFs compared with poly[carbazole-*alt*-benzothiadiazole] (PCZDTB).

INTRODUCTION

For the past several decades, semiconducting polymers have been applied to various sectors, such as organic light emitting diodes (OLEDs),[1−4] organic photovoltaic cells (OPVs)[5−9] and organic thin film transistors (OTFTs).[10−13] Of these applications, OPVs have become mainstream, thanks to their outstanding economic feasibility and sustainable development. Nevertheless, a low power conversion efficiency (PCE) has been the largest obstacle in OPVs.[6] To improve the PCE, the following idealistic conditions are required in conjugated polymers:[14] (1) a low bandgap with a wide absorption area, (2) a crystalline structure to produce good charge transport characteristics, (3) a low highest occupied molecular orbital (HOMO) energy level to produce a high open-circuit voltage (V_{oc}), and (4) an appropriate lowest unoccupied molecular orbital (LUMO) energy level for effective electron charge transfer to fullerene.

To acquire good charge transport characteristics, it is necessary to increase the close packing among polymers through the reduction of energetic disorder by increasing the coplanarity and the interchain $\pi-\pi$ interaction. In the Janssen group, a copolymer containing terthiophene was reported, which shows an increase in planarity packing and high mobility characteristics, and a diketopyrrolopyrrole derivative showed a PCE of 4.7% and a high hole mobility (0.04 $cm^2\ V^{-1}\ S^{-1}$).[15] In the Jen group, a hole mobility of 0.029 $cm^2\ V^{-1}\ S^{-1}$ and a PCE of 6.2% were reported in a copolymer that contained an indacenodithiophene (IDT) unit and a phenanthrenequinoxaline unit.[16] In the McCulloch group, in addition, a hole mobility of 0.24 $cm^2\ V^{-1}\ S^{-1}$ and a PCE of 2.2% were reported in a polymer containing

Received: July 15, 2012
Revised: September 8, 2012
Published: September 18, 2012

Scheme 1. Scheme of Monomer Synthesis and Polymerization

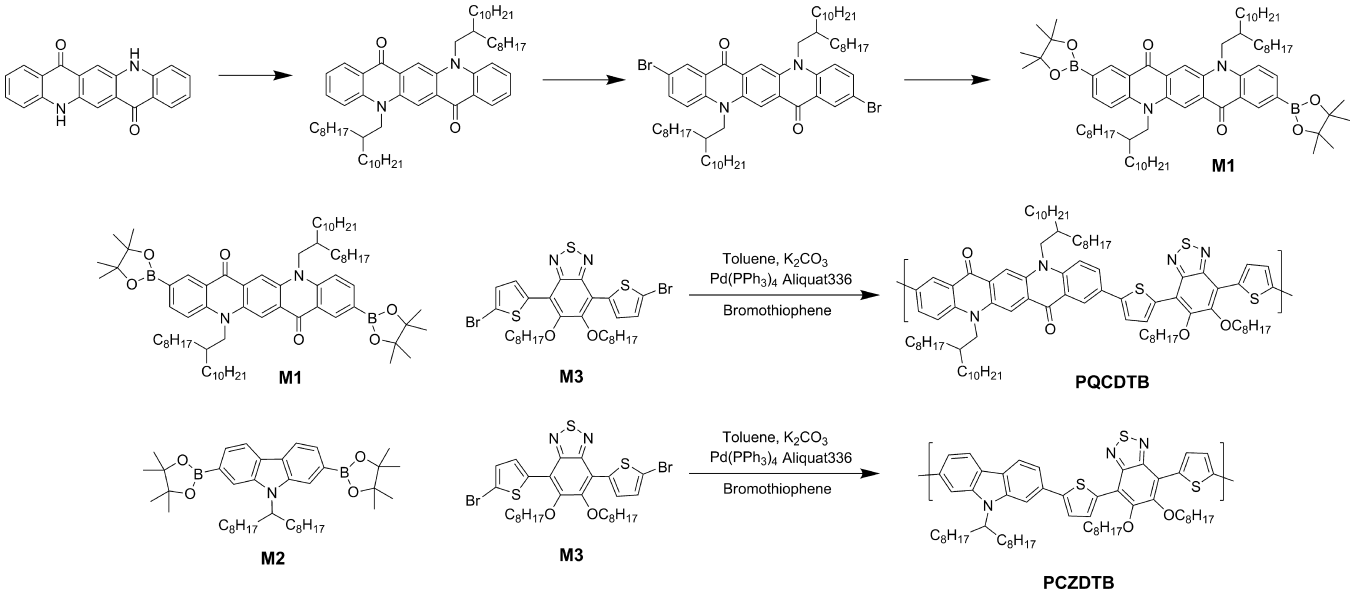

benzo[1,2-*b*:3,4-*b*′:5,6-*d*′]trithiophene (BTT) to produce effective intermolecular packing characteristics.[17,18]

Quinacridone (QC) derivative, which is known as a red-violet pigment, has a high crystallinity and self-assembled characteristics, so it has drawn significant attention as an OTFT because of its high mobility.[19,20] However, these QC results were primarily reported for small molecules or oligomers. In the case of polymers, extremely limited results have been reported.[21,22] In the Takimiya group, recently, a polymer composed of QC derivatives has been reported for use in OTFTs that has a high hole mobility (0.2 $cm^2 V^{-1} S^{-1}$).[23]

In this study, we synthesized a new donor−acceptor type (D−A type) polymer, poly[quinacridone-*alt*-octyloxydithienylbenzothiadiazole] (PQCDTB), which contained QC and octyloxydithienylbenzothiadiazole (DTB). As a result, it is most likely that a broad absorbance could be obtained as the results of the effective charge transport and the strong electron-withdrawing caused by the high coplanarity.

RESULTS AND DISCUSSION

Scheme 1 reveals the chemical structure and synthetic process for both the monomer and the polymer. As shown in this scheme, PQCDTB was synthesized through the Suzuki coupling reaction using M1 and M3, while poly[carbazole-*alt*-octyloxydithienylbenzothiadiazole] (PCZDTB) was synthesized using M2 and M3. The polymerization was carried out at 90 °C for 24 h with palladium catalyst (0), 2 M potassium carbonate solution, aliquot 336 as a surfactant, and toluene as the solvent. After the polymerization was over, it was end-capped with bromothiophene. The synthesized polymer was purified with Soxhlet extraction in the following order: methanol, acetone and chloroform. Then, the polymer was recovered from the chloroform fraction and precipitated into methanol. As a result, the yields of PQCDTB and PCZDTB reached 92% and 72%, respectively. The obtained polymer dissolved in organic solvents, such as THF, chloroform, chlorobenzene and *o*-dichlorobenzene. Through spin-coating, a homogeneous and violet semitransparent film was formed.

Table 1 shows the result of the molecular weight and the thermal properties of the obtained PQCDTB. As shown in this table, when the GPC was measured using polystyrene as the standard, the number-average molecular weights (M_n) of PQCDTB and PCZDTB were 49.8 and 15.2 kg/mol, respectively. In contrast, the polydispersity indices (PDIs) showed a very narrow distribution of 1.92 and 1.77, respectively. In terms of the degree of polymerization, PQCDTB was greater than other OPV polymers by 2−3 times because of the introduction of long, branched side chains of quinacridone and benzothiadiazole. As a result, the backbone structure became relatively favorable in terms of the solubility at polymerization; polymerization had effectively occurred.[6] Table 1 showed the result of the thermal analysis through TGA. As shown in Table 1, PQCDTB and PCZDTB had a 5% weight loss at the temperatures of 323 and 324 °C, respectively, displaying a high thermal stability because of the rigid QC and carbazole structure, which is applicable for optoelectronic devices and OPVs, both of which require a high thermal stability (300 °C or above).[24] We investigated thermal behavior through DSC analysis (see Supporting Information), which revealed no obvious thermal transitions for PQCDTB in the temperature range from 40 to 250 °C. Thus, PQCDTB displayed amorphous property.

Table 1. Molecular Weight and Thermal Properties of Polymers

polymer	M_n (kg/mol)	M_w (kg/mol)	PDI	T_d (°C)
PQCDTB	49.8	96.0	1.92	323
PCZDTB	15.2	26.9	1.77	324

Figure 1 showed X-ray diffraction measurements of film to analyze the ordering structure of the obtained polymers. In the out-of-plane of PQCDTB, as shown Figure 1a, a sharp diffraction peak was observed at 4.0, 8.1, 12.2°, which indicates the formation of ordered lamellar structure as an out-of-plane peak (*h*00) by the alkyl side chain of quinacridone and conventional edge-on π- stacking.[5,14,23] The lamellar *d*-spacing (d_1) was 21.8 Å ($\lambda = 2d[\sin\theta]$). In the (010) in-plane pattern related to $\pi-\pi$ stacking, as shown Figure 1b, a broad diffraction peak was detected at approximately 24.0°. Using the same calculation, the $\pi-\pi$ stacking distance (d_π) was 3.7 Å. The results are similar to thiophene and thiophene-fused aromatic system polymers that

dx.doi.org/10.1021/ma301466m | *Macromolecules* 2012, 45, 7815−7822

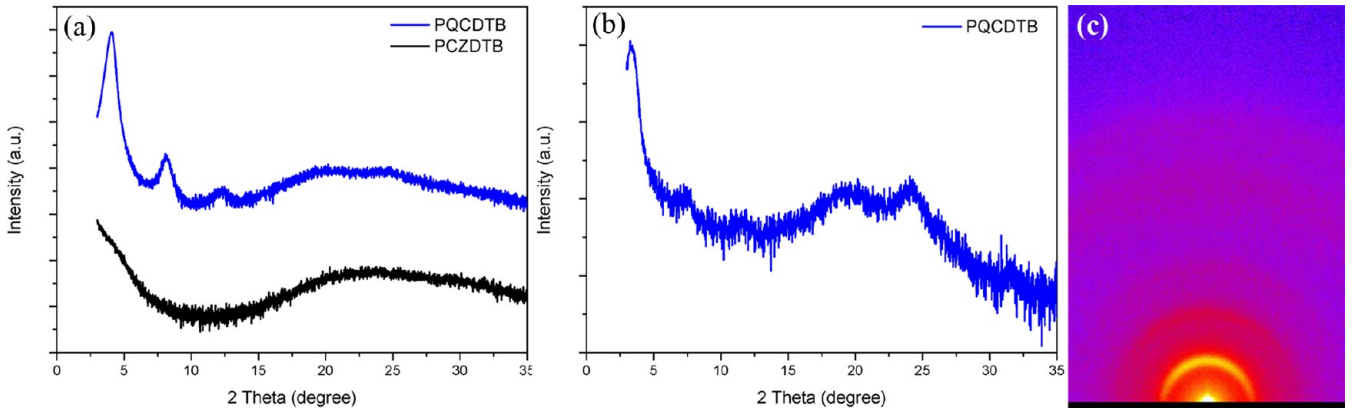

Figure 1. (a) Out-of-plane, (b) in-plane, and (c) 2D-GIXD image X-ray diffraction pattern of annealed polymer in thin films.

perform well as OPVs.[19,25] In the out-of-plane of PCZDTB, as shown in Figure 1a, no diffraction peak was observed in the thin film. As reported before, a broad diffraction peak was observed at approximately 20.5° in the diffraction of powdery PCZDTB (see Supporting Information).[26] The $\pi-\pi$ stacking distance (d_π) was 4.3 Å. The result was similar to the result for $\pi-\pi$ stacking (d_π = 4.0−4.4 Å) of fluorene-thiophene. The benzene-thiophene linkage has a twisted structure compared with the thiophene-thiophene linkage. The structure has an impact on $\pi-\pi$ stacking (d_π) as well.[27] By calculating PCZDTB and PQCDTB using a density functional theory (DFT) calculation, the tilt angle has been comparatively analyzed. In terms of tilt angle, PCZDTB was 27−28°, while PQCDTB was 19−21°. Compared with PCZDTB, formation of a planar backbone and stronger $\pi-\pi$ stacking were observed in PQCDTB (see Supporting Information). On the basis of this result, it has been confirmed that $\pi-\pi$ stacking was more effective in PQCDTB than in PCZDTB because of coplanarity of the quinacridone unit that was introduced to the main chain of PQCDTB.[13]

Figure 2 showed the UV−visible spectra of PQCDTB and PCZDTB. As shown in Figure 2, the maximum absorption peak of PQCDTB (λ_{max}) was observed at 389 and 539 nm, respectively, in solution (10^{-6} M in chloroform). On the other hand, the maximum absorption peaks of PCZDTB (λ_{max}) were observed at 386 and 514 nm in solution. The band around 380 nm in the absorption spectra of PQCDTB and PCZDTB can be assigned to $\pi-\pi^*$ transition whereas the 530−550 band are due to intramolecular charge transfer (ICT) between donor and acceptor moieties.[10] The absorption spectrum of PQCDTB is broadened and red-shifted compared to that of PCZDTB. This can be explained by the much stronger ICT effects in the PQCDTB than that in PCZDTB. For the film, the maxima absorption spectra of PQCDTB and PCZDTB were red-shifted by 9−23 nm compared with the solution. These results are explained by their much more planar conformations in the solid state.[10]

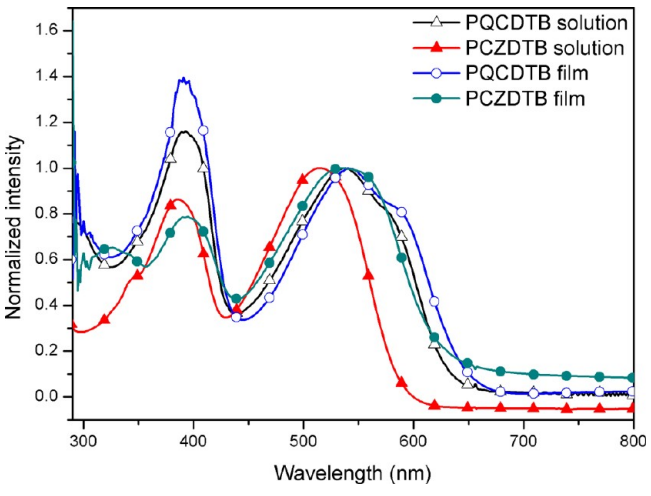

Figure 2. Absorption spectra of PQCDTB and PCZDTB in solution (10^{-6} M) and film (50 nm).

Figure 3 shows the cyclic voltammogram of PCZDTB and PQCDTB, which were measured in 0.1 M tetrabutylammonium-hexafluorophosphate acetonitrile. As reported by Lidzey et al., the PCZDTB oxidation (E_{ox}^{onset}) and reduction (E_{red}^{onset}) onset potential were +1.09 and −1.37 V, respectively, and the HOMO and LUMO levels were −5.44 and −2.98 eV. In the case of PQCDTB, unlike the PQA2T (poly[quinacridone−bithiophene]) reported by Takimiya et al., a clear oxidation−reduction peak was observed.[19] This type of result has been obtained because PQCDTB was D−A structured, unlike the typical p-type structure of PQA2T. In PQCDTB, the oxidation (E_{ox}^{onset}) and reduction (E_{red}^{onset}) onset potentials were +0.89 and −1.36 V, respectively. The HOMO and LUMO levels were −5.24 and −2.99 eV, respectively.

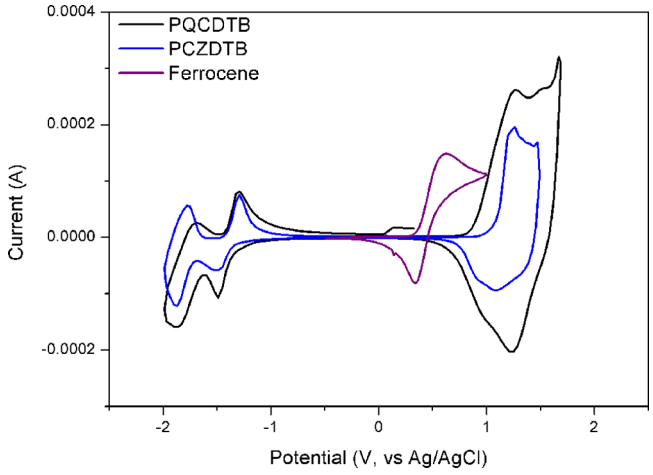

Figure 3. Cyclic voltammogram of PQCDTB and PCZDTB.

Table 2 summarizes the optical and electrochemical properties of polymers. As shown in Table 2, the HOMO level of PQCDTB (−5.24 eV) was higher than that of PCZDTB by 0.2 eV because

dx.doi.org/10.1021/ma301466m | Macromolecules 2012, 45, 7815−7822

Table 2. Optical and Electrochemical Properties of Polymers

	absorption, λ_{max} (nm)					
polymer	solution[a]	film[b]	E_{HOMO}(eV)[c]	E_{LUMO}(eV)[c]	E_{LUMO}(eV)[d]	E_{opt}(eV)[e]
PQCDTB	389, 539	391, 548	−5.24	−2.99	−3.32	1.92
PCZDTB	386, 514	395, 537	−5.44	−2.98	−3.46	1.98

[a]Absorption spectrum in chloroform solution (10^{-6} M). [b]Spin-coated thin film (50 nm). [c]Calculated from the oxidation or reduction onset potentials under the assumption that the absolute energy level of Fc/Fc^+ was −4.8 eV below a vacuum. [d]HOMO − E_{opt}. [e]Estimated from the onset of UV−vis absorption data of the thin film.

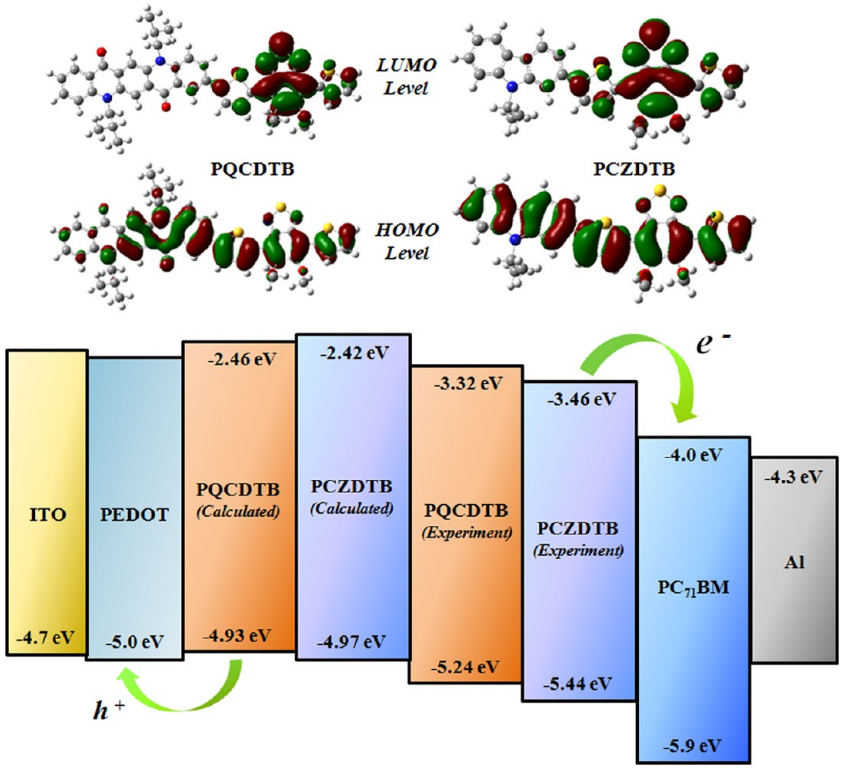

Figure 4. Band diagram of PQCDTB and PCZDTB (calculated and experiment level).

the HOMO level of the QC derivative was higher than that of carbazole. The LUMO energy levels were calculated from the difference between the HOMO energy levels and the optical bandgap energies. According to the calculations, the LUMO levels of PQCDTB and PCZDTB were −3.32 and −3.46 eV, respectively. They slightly differed from the levels calculated through CV, but they mostly exhibited a similar tendency. Figure 4 shows the band diagram of the energy levels that have been obtained through DFT calculations and experiments. The bandgap energies of PQCDTB and PCZDTB determined through UV−vis spectra were reported as 1.98 and 1.92 eV, respectively, which were lower than the results of the DFT calculation by 0.57 and 0.55 V.[28] Because the HOMO level is lower than the P3HT HOMO level (−4.9 eV) in both polymers, a relatively high air stability could be obtained.[29] In the case of PQCDTB, the LUMO level (−3.32 eV) was higher than the $PC_{71}BM$ LUMO level (−4.0 eV) by 0.68 eV. However, the HOMO level (−5.24 eV) was lower than the PEDOT:PSS HOMO level (−5.0 eV) by 0.24 eV. Therefore, if charge separation occurs after receiving light energy, a hole would exhibit more effective charge transport than an electron in the active layer of PQCDTB.[14,26]

Figure 5 and Table 3 show the results of evaluating the characteristics of an OPV device. The devices are structured as follows: ITO (170 nm)/PEDOT:PSS (40 nm)/active layer (50 nm)/BaF_2 (2 nm)/Ba (2 nm)/Al (100 nm). The active layer has an optimized blending ratio obtained by dissolving polymer and PCBM in o-dichlorobenzene (ODCB) with a 0.5−1 wt % concentration. The photovoltaic performances of the fabricated OPVs were investigated under AM 1.5G simulated solar light at 100 mW cm^{-2}.

As shown in Figure 5a and Table 3, the device that blended PQCDTB and $PC_{61}BM$ in a 1:1 ratio had an open-circuit voltage (V_{OC}) of 0.76 V, a short-circuit current (J_{SC}) of 4.4 mA cm^{-2}, a fill factor (FF) of 47.5% and a power conversion efficiency (PCE) of 1.6%. In the device that blended the PQCDTB and $PC_{71}BM$ in a 1:1 ratio, V_{OC}, J_{SC}, and FF were 0.79 V, 5.6 mA cm^{-2}, and 55.8%, respectively. In terms of PCE, approximately 56% was improved with 2.5%, compared with the device in which the $PC_{61}BM$ was applied as an acceptor. Because $PC_{71}BM$ is greater than $PC_{61}BM$ in terms of photon absorption at 400−500 nm, it was able to improve the PCE by increasing J_{SC}.[6] The V_{oc} of PQCDTB was greater than the widely known poly(3-hexylthiophene), P3HT (V_{oc} = 0.5−0.6 V). This type of result was obtained because PQCDTB (−5.53 eV) has a lower HOMO level than P3HT (−4.9 eV).[19,24] The value of FF for PQCDTB (FF = 55.8%) increased by 39% compared to PCZDTB (FF = 40.1%). The series resistance at PQCDTB and $PC_{71}BM$ ratios of 1:1 and 1:2,

dx.doi.org/10.1021/ma301466m | Macromolecules 2012, 45, 7815−7822

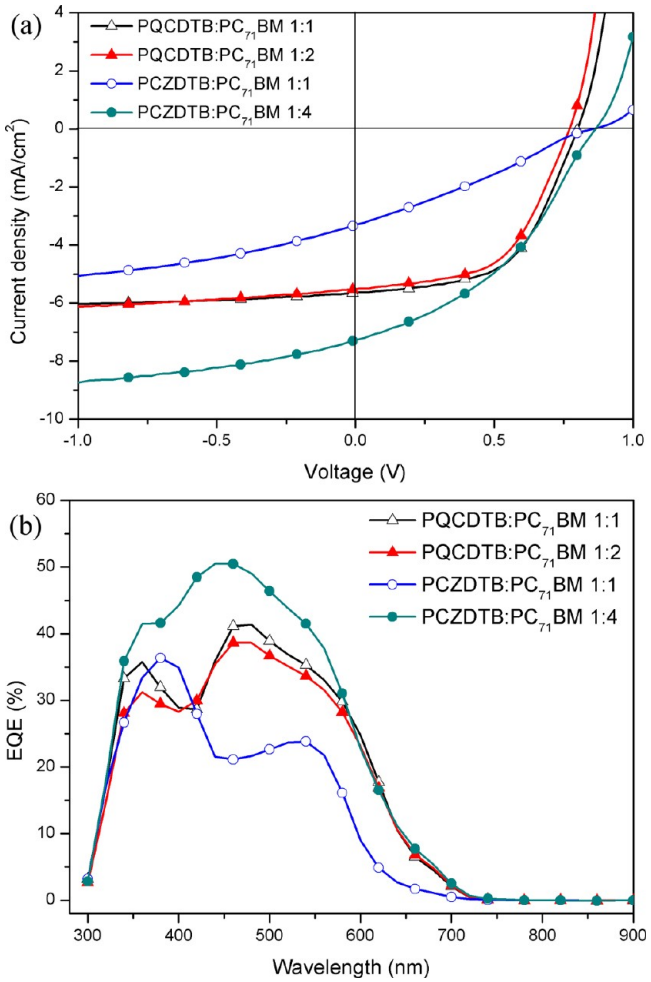

Figure 5. (a) $J-V$ characteristics; (b) EQE spectra of the BHJ solar cells with the device.

as shown in Table 3, was 31 and 27 Ω/cm^2, respectively. In contrast, the series resistance at PCZDTB and $PC_{71}BM$ ratio of 1:1 and 1:4 was 320, 62 Ω/cm^2, respectively. The series resistance of PQCDTB exhibited low value compared to that of PCZDTB. The decrease of series resistance could increase FF. PQCDTB showed high FF than PCZDTB due to decrease of series resistance by self-organization of quinacridone unit.[9]

Figure 5b showed the external quantum efficiency (EQE) data of the fabricated device. When PQCDTB was used as a donor and $PC_{61}BM$ and $PC_{71}BM$ were used as acceptors, the device had 38% and 41% EQE at 480 nm, respectively. The photovoltaic devices with $PC_{71}BM$ as an acceptor showed higher EQE values than those with $PC_{61}BM$ as an acceptor, although they absorbed photons in the same range of the solar spectra. This was because $PC_{71}BM$ has a stronger UV−vis absorption property than does $PC_{61}BM$ in the visible region, especially near 500 nm.[30] Hence, the PCE improved with an increase in J_{SC}. In a device that used PCZDTB as a donor, an EQE of 48% was observed at 440 nm. Interestingly, λ_{max} was blue-shifted by −30 nm because of the low $\pi-\pi$ stacking and the weak intermolecular interaction of PCZDTB compared with PQCDTB.

To investigate the morphology of the polymer/PCBM blend film, atomic force microscopy (AFM) was performed, and the result is shown in Figure 6. In Figure 6a, microphase separation occurred between the polymer and $PC_{71}BM$, while the polymer formed a small fibril-type domain at a 1:1 PQCDTB/$PC_{71}BM$ ratio. As shown in Figure 6c, the fibril domain or microphase separation was clearer when measured at a 1 × 1 μm^2 size. It appears that this type of fibril domain occurred because PQCDTB formed effective $\pi-\pi$ stacking based on outstanding crystallinity.[31] As shown in Figure 6b, in contrast, when the PQCDTB/$PC_{71}BM$ ratio was 1:2, the polymers were assembled, and a large domain was formed. As a result, a relatively large-size phase separation took place. As shown in Figure 6d, the large domain or the large-size phase separation was clearer when measured at a 1 × 1 μm^2 size. The large-phase separation exhibits a low photocurrent by reducing the charge separation and increasing the exciton diffusion length and the recombination of electric charges.[32] Therefore, at a 1:2 polymer/$PC_{71}BM$ ratio, a large phase separation occurs between the polymer and the $PC_{71}BM$. As a result, a low photocurrent would occur; this is comparable to the 1:1 ratio. The same results were confirmed for the current device using the data in Table 3. Similar results were observed between PQCDTB and $PC_{61}BM$ as well. When the PCZDTB:PC71BM ratio was 1:4, a smooth morphology was detected, and no fibril domain was observed, just like the PQCDTB, because the self-organization of PCZDTB is lower than that of PQCDTB.[9]

CONCLUSION

In this study, PQCDTB has been successfully synthesized through the Suzuki coupling reaction by introducing planar quinacridone unit and a broad-absorption benzothiadiazole unit. PQCDTB had a high molecular weight and good thermal stability. Because of the appropriate HOMO and LUMO energy levels, an effective balance was produced. According to the X-ray diffraction measurement, a broad diffraction peak was observed at approximately 24.0°. In terms of the $\pi-\pi$ stacking distance (d_π), a significantly shorter distance (3.7 Å) was observed. These values were similar to the results of the thiophene and thiophene-fused aromatic system polymers. When the PQCDTB:$PC_{71}BM$ ratio was 1:1, the highest efficiency was detected, and V_{OC}, J_{SC}, FF, and PCE were 0.79 V, 5.6 mA cm^{-2}, 55.8%, and 2.5%, respectively. When the PQCDTB:PC71BM ratio was 1:1, the polymer formed a fibril-type domain and microphase separation occurred between the polymer and $PC_{71}BM$. Because of self-organization, PQCDTB showed a higher FF compared with PCZDTB. It is likely that more effective performance levels could

Table 3. Photovoltaic Performance of the BHJ Solar Cells with the Device

active layer (w/w)								
polymer (P)	acceptor (A)	weight ratio (P:A, w/w)	V_{OC} (V)	J_{SC} (mA/cm^2)	FF (%)	PCE (%)	R_s (Ω/cm^2)	R_{sh} (Ω/cm^2)
PQCDTB	$PC_{71}BM$	1:1 (50 nm)	0.79	5.6	55.8	2.5	31	1483
		1:2 (50 nm)	0.77	5.5	54.6	2.3	27	1115
PCZDTB	$PC_{71}BM$	1:1 (50 nm)	0.85	3.3	28.2	0.8	320	368
		1:4 (50 nm)	0.85	7.2	40.1	2.5	62	401

dx.doi.org/10.1021/ma301466m | Macromolecules 2012, 45, 7815−7822

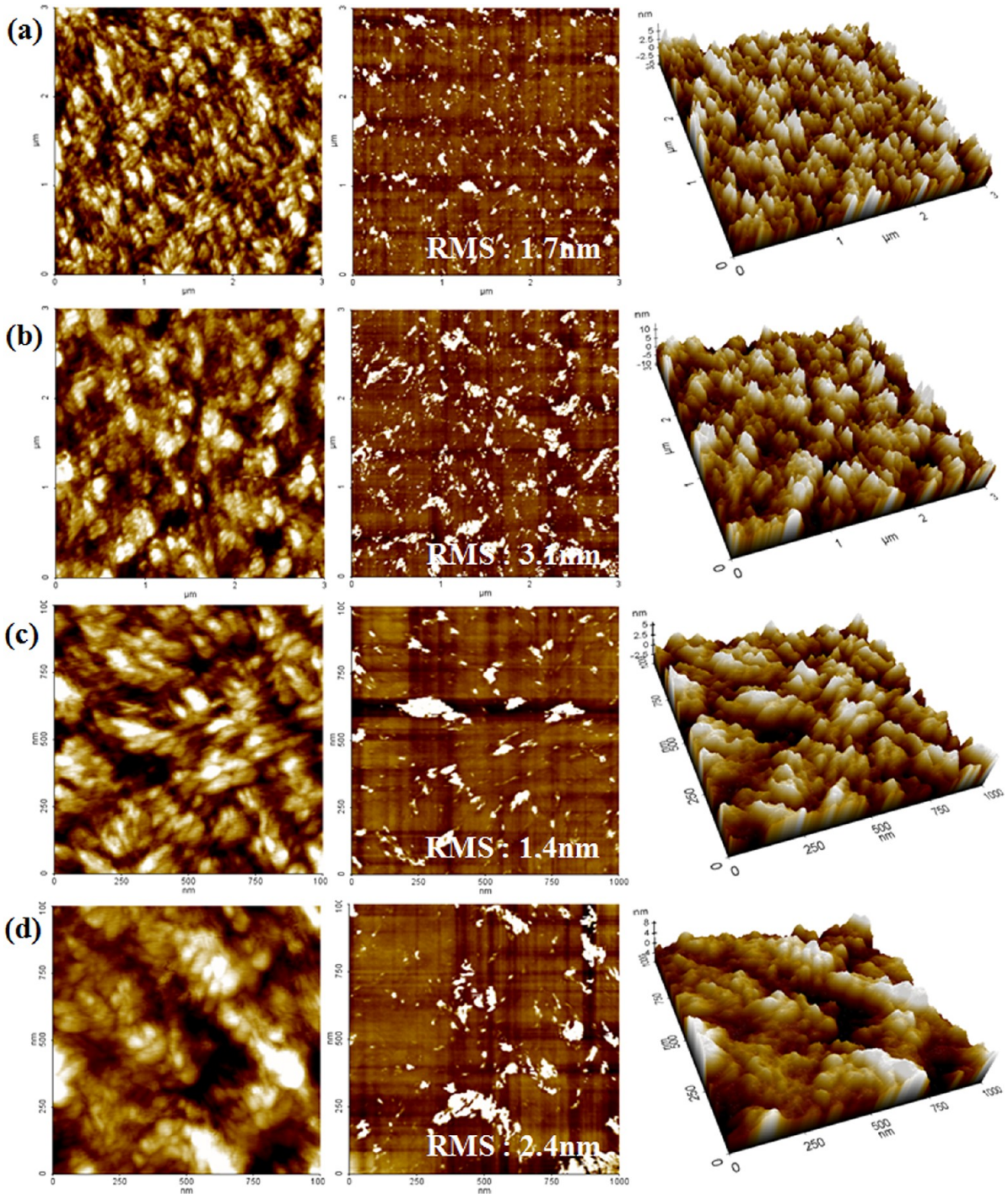

Figure 6. Topographic AFM images of (a) PQCDTB:$PC_{71}BM$ 1:1 ($3 \times 3\ \mu m^2$), (b) PQCDTB:$PC_{71}BM$ 1:2 ($3 \times 3\ \mu m^2$), (c) PQCDTB:$PC_{71}BM$ 1:1 ($1 \times 1\ \mu m^2$), and (d) PQCDTB:$PC_{71}BM$ 1: 2 ($1 \times 1\ \mu m^2$).

be obtained if the chemical structure and device structure of the polymer were optimized.

EXPERIMENTAL SECTION

Instruments and Characterization. Unless otherwise specified, all the reactions were carried out under nitrogen atmosphere. Solvents were dried by standard procedures. All column chromatography was performed with the use of silica gel (230−400 mesh, Merck) as the stationary phase. ^1H NMR spectra were performed in a Bruker ARX 400 spectrometer using solutions in $CDCl_3$ and chemical were recorded in ppm units with TMS as the internal standard. The elemental analyses were measured with EA1112 using a CE Instrument. Electronic absorption spectra were measured in chloroform using a HP Agilent 8453 UV−vis spectrophotometer. The cyclic voltammetric waves were produced using a Zahner IM6eX electrochemical workstation with a 0.1 M acetonitrile (substituted with nitrogen for 20 min) solution containing tetrabutyl ammonium hexafluorophosphate (Bu_4NPF_6) as the electrolyte at a constant scan rate of 50 mV/s. ITO, a Pt wire, and silver/silver chloride [Ag in 0.1 M KCl] were used as the working, counter, and reference electrodes, respectively. The electrochemical potential was calibrated against Fc/Fc^+. The HOMO levels of the polymers were determined using the oxidation onset value. Onset potentials are values obtained from the intersection of the two tangents drawn at the rising current and the baseline changing current of the CV

dx.doi.org/10.1021/ma301466m | *Macromolecules* 2012, 45, 7815−7822

curves. TGA measurements were performed on NETZSCH TG 209 F3 thermogravimetric analyzer. All GPC analyses were made using THF as eluant and polystyrene standard as reference. X-ray diffraction (XRD) patterns were obtained using SmartLab 3 kW (40 kV 30 mA, Cu target, wavelength: 1.541871 ang), Rigaku, Japan. 2D-GIXRD: CBO-f (point-like beam optic), PILATUS 100 K−S (2D detector). Topographic images of the active layers were obtained through atomic force microscopy (AFM) in tapping mode under ambient conditions using a XE-100 instrument. Theoretical study was performed by using density functional theory (DFT), as approximated by the B3LYP functional and employing the 6-31G* basis set in Gaussian09.

Fabrication and Characterization of Polymer Solar Cells. All of the bulk-heterojunction PV cells were prepared using the following device fabrication procedure. The glass/indium tin oxide (ITO) substrates [Sanyo, Japan (10 Ω/γ)] were sequentially lithographically patterned, cleaned with detergent, and ultrasonicated in deionized water, acetone, and isopropyl alcohol. Then the substrates were dried on a hot-plate at 120 °C for 10 min and treated with oxygen plasma for 10 min in order to improve the contact angle just before the film coating process. Poly(3,4-ethylene−dioxythiophene):poly(styrene−sulfonate) (PEDOT:PSS, Baytron P 4083 Bayer AG) was passed through a 0.45 μm filter before being deposited onto ITO at a thickness of ca. 32 nm by spin-coating at 4000 rpm in air and then it was dried at 120 °C for 20 min inside a glovebox. Composite solutions with polymers and PCBM were prepared using 1,2-dichlorobenzene (DCB). The concentration was controlled adequately in the 0.5 wt % range, and the solutions were then filtered through a 0.45 μm PTFE filter and then spin-coated (500−2000 rpm, 30 s) on top of the PEDOT:PSS layer. The device fabrication was completed by depositing thin layers of BaF_2 (1 nm), Ba (2 nm), and Al (200 nm) at pressures of less than 10^{-6} Torr. The active area of the device was 4.0 mm^2. Finally, the cell was encapsulated using UV-curing glue (Nagase, Japan). In this study, all of the devices were fabricated with the following structure: ITO glass/PEDOT:PSS/polymer:PCBM/ BaF_2/ Ba/Al/encapsulation glass.

The illumination intensity was calibrated using a standard a Si photodiode detector that was equipped with a KG-5filter. The output photocurrent was adjusted to match the photocurrent of the Si reference cell in order to obtain a power density of 100 mW/cm^2. After the encapsulation, all of the devices were operated under an ambient atmosphere at 25 °C. The current−voltage (I−V) curves of the photovoltaic devices were measured using a computer-controlled Keithley 2400 source measurement unit (SMU) that was equipped with a Peccell solar simulator under an illumination of AM 1.5G (100 mW/cm^2). Thicknesses of the thin films were measured using a KLA Tencor Alpha-step 500 surface profilometer with an accuracy of 1 nm.

Synthesis. All reagents were purchased from Aldrich, Acros, or TCI companies. All chemicals were used without further purification. The following compounds were synthesized following modified literature procedures: 4,7-bis(5-bromothiophen-2-yl)-5,6-bis(octyloxy)-benzothiadiazole (M3) and poly[carbazole-*alt*-octyloxydithienylbenzo-thiadiazole] (PCZDTB).[8]

***N,N′*-Di(2-octyldodecyl)quinacridone.** Quinacridone (4.0 g, 13.0 mmol) and KOH (19.6 g, 351 mmol) were dissolved in DMF (50 mL). The mixture was stirred for 30 min, followed by addition of 9-(bromomethyl)nonadecane (28.6 g, 71.9 mmol). The resulting mixture was heated to a reflux for 24 h. After cooling, the mixture was poured into water (50 mL), extracted with ethyl acetate (EA), and then dried over Na_2SO_4. The solvent was removed by rotary evaporation, and the resulting crude product was purified by column chromatography eluting with dichloromethane yielding the product as red solid. (0.7 g, 7%). ^{1}H NMR (400 MHz; $CDCl_3$; Me_4Si): 8.89 (s, 2H), 8.61 (d, 2H), 7.77 (t, 2H), 7.61 (d, 2H), 7.29 (t, 2H), 4.54 (s, 4H), 2.28 (m, 2H), 1.51−1.11 (m, 64H), 0.87−0.84 (t, 12H). ^{13}C NMR (100 MHz; $CDCl_3$; Me_4Si): 178.0, 142.9, 136.3, 134.2, 128.1, 126.1, 121.2, 120.8, 115.4, 114.4, 49.8, 36.8, 31.8(4), 29.5(9), 22.6(2), 14.1(2) Anal. Calcd for $C_{60}H_{92}N_2O_2$: C, 82.51; H, 10.62; N, 3.21; O, 3.66. Found: C, 82.06; H, 11.28; N, 2.85; O, 4.16.

2,9-Dibromo-*N,N′*-di(2-octyldodecyl)quinacridone. The mixture of *N,N′*-Di(2-octyldodecyl)quinacridone (1.7 g, 1.94 mmol) and sodium acetate (0.41 g, 5.04 mmol) and acetic acid (80 mL) was heated to reflux with stirring. A solution of Br_2 (1.09 g, 6.8 mmol) in acetic acid (10 mL) was added dropwise to the mixture, followed by stirring for 1 h. After the mixture had cooled, the precipitated solid was collected by filtration and washed with aqueous $NaHSO_3$ and water. The crude product was recrystallized in hexane the product as red solid. (1.12 g, 55%) ^{1}H NMR (400 MHz; $CDCl_3$; Me_4Si): 8.75 (s, 2H), 8.63 (d, 2H), 7.76 (dd, 2H), 7.45 (d, 2H), 4.45 (s, 4H), 2.19 (m, 2H), 1.53−1.21 (m, 64H), 0.90−0.84 (t, 12H). ^{13}C NMR (100 MHz; $CDCl_3$; Me_4Si): 176.0, 141.3, 136.8, 130.1, 121.9, 117.5, 114.5, 114.0, 49.8, 36.8, 31.8(4), 29.5(9), 22.6(2), 14.1(2) Anal. Calcd for $C_{60}H_{90}Br_2N_2O_2$: C, 69.89; H, 8.80; N, 2.72; O, 3.10. Found: C, 67.20; H, 8.90; N, 2.72; O, 3.53.

2,9-Diboronic Ester-*N,N′*-di(2-octyldodecyl)quinacridone (M1). A solution of 2,9-dibromo-*N,N′*-di(2-octyldodecyl)quinacridone (1.0 g, 0.96 mmol), bis(pinacolato)diboron (0.55 g, 2.20 mmol), $PdCl_2$(dppf) (0.12 g, 0.16 mmol) and KOAc (0.54 g, 5.57 mmol) in degassed 1,4-dioxane (10 mL) was stirred at 80 °C overnight. The reaction was quenched by adding water, and the resulting mixture was washed with chloroform. The organic layers were washed with brine, dried over Na_2SO_4. The solvent was removed by rotary evaporation, and the crude product was recrystallized in ethyl acetate (EA) the product as brown solids. (0.74 g, 67%) ^{1}H NMR (400 MHz; $CDCl_3$; Me_4Si): 9.07 (s, 2H), 8.87 (d, 2H), 8.11 (dd, 2H), 7.56 (d, 2H), 4.52 (s, 4H), 2.24 (m, 2H), 1.43 (s, 24H), (1.38−1.11 m, 64H), 0.90−0.84 (t, 12H). ^{13}C NMR (100 MHz; $CDCl_3$; Me_4Si): 179.8, 144.6, 139.6, 136.1, 127.4, 120.4, 114.8, 114.0, 83.9, 49.8, 36.8, 31.8(4), 29.5(9), 22.6(2), 14.1(2) Anal. Calcd for $C_{72}H_{114}B_2N_2O_6$: C, 76.85; H, 10.21; N, 2.49; O, 8.53. Found: C, 75.71; H, 10.42; N, 2.26; O, 6.74.

Poly[quinacridone-*alt*-octyloxydithienylbenzothiadiazole] (PQCDTB). 4,7-Bis(5-bromothiophen-2-yl)-5,6-bis(octyloxy)-benzothiadiazole (M3) (0.19 g, 0.27 mmol), 2,9-diboronic ester-*N,N′*-di(2-octyl-dodecyl)quinacridone (M1) (0.30 g, 0.27 mmol), Pd-$(PPh_3)_4$(0) (0.009 g, 0.008 mmol) and aliquat336, were placed in a Schlenk tube, purged with three nitrogen/vacuum cycles, and under nitrogen atmosphere added 2 M degassed aqueous K_2CO_3 (10 mL) and dry toluene(20 mL). The mixture was heated to 90 °C and stirred in the dark for 24 h. After the polymerization was over, it was end-capped with bromothiophene. After reaction quenching, the whole mixture was poured into methanol. The precipitate was filtered off, purified with Soxhlet extraction in the following order: methanol, acetone and chloroform. The polymer was recovered from the chloroform fraction and precipitated into methanol. The final product was obtained after drying in vacuum as a dark black solid. (0.36 g, 92%) Anal. Calcd for $C_{90}H_{130}N_4O_4S_3$: C, 75.69; H, 9.17; N, 3.92; S, 6.74; O, 4.48. Found: C, 74.61; H, 9.07; N, 3.81; S, 6.03; O, 5.36.

■ ASSOCIATED CONTENT

Ⓢ Supporting Information

^{1}H NMR and ^{13}C NMR of M1, TGA data of PQCDTB and PCZDTB, DSC data of PQCDTB, X-ray diffraction pattern of powdery PQCDTB and PCZDTB, dihedral angle of PQCDTB and PCZDTB, topographic AFM images of PCZDTB:$PC_{71}BM$, and photovoltaic performance of the BHJ solar cells with the device. This material is available free of charge via the Internet at http://pubs.acs.org.

■ AUTHOR INFORMATION

Corresponding Author

*E-mail: dkmoon@konkuk.ac.kr.

Notes

The authors declare no competing financial interest.

■ ACKNOWLEDGMENTS

This research was supported by a grant from the Fundamental R&D Program for Core Technology of Materials funded by the Ministry of Knowledge Economy, Republic of Korea. This work was supported by the National Research Foundation of Korea Grant funded by the Korean Government(MEST) (NRF-2009-

C1AAA001-2009-0093526). We appreciate the help of Dr. Se-Jeong Park (Korea ITS Co. Ltd.). 2D-GIXRD experiments were performed with her at the laboratory of Korea ITS Co. Ltd.

REFERENCES

(1) Friend, R. H.; Gymer, R. W.; Holmes, A. B.; Burroughes, J. H.; Marks, R. N.; C. Taliani, C.; Bradley, D. D. C.; Dos Santos, D. A.; Bredas, J. L.; Logdlund, M.; Salaneck, W. R. *Nature (London)* **1999**, *397*, 121−128.
(2) Breen, C. A.; Tischler, J. R.; Bulovic, V.; Swager, T. M. *Adv. Mater.* **2005**, *17*, 1981−1985.
(3) Song, H. J.; Lee, J. Y.; Song, I. S.; Moon, D. K.; Haw, J. R. *J. Ind. Eng. Chem.* **2011**, *17*, 352−357.
(4) Guo, X.; Qin, C.; L.; Cheng, I.; Xei, Z.; Geng, Y.; Jing, X.; Wang, F.; Wang, L. *Adv. Mater.* **2009**, *21*, 3682−3688.
(5) Subramaniyan, S.; Xin, H.; Kim, F. S.; Shoaee, S.; Durrant, J. R.; Jenekhe, S. A. *Adv. Energy Mater.* **2011**, *1*, 854−860.
(6) Lee, J. Y.; Kim, S. H.; Song, I. S.; Moon, D. K. *J. Mater. Chem.* **2011**, *21*, 16480−16487.
(7) Zhang, Z. G.; Wang, J. *J. Mater. Chem.* **2012**, *22*, 4178−4187.
(8) Yi, H.; Al-Faifi, S.; Iraqi, A.; Watters, D. C.; Kingsley, J.; Lidzey, D. G. *J. Mater. Chem.* **2011**, *21*, 13649−13656.
(9) Li, G.; Shrotriya, V.; Huang, J.; Yao, Y.; Moriarty, T.; Emery, K.; Yang, Y. *Nature materials* **2005**, *4*, 864−868.
(10) Zhu, Y.; Champion., R. D.; Jenekhe., S. A. *Macromolecules* **2006**, *39*, 8712−8719.
(11) Mcculloch, I.; Heeney, M.; Bailey, C.; Genevicius, K.; Macdonald, I.; Shkunov, M.; Sparrowe, D.; Tierney, S.; Wagner, R.; Zhang, W.; Chabinyc, M. L.; Kline, R. J.; Mcgehee, M. D.; Toney, M. F. *Nature: Mater.* **2006**, *5*, 328−333.
(12) Mei, J.; Kim, D. H.; Ayzner, A. L.; Toney, M. F.; Bao, Z. *J. Am. Chem. Soc.* **2011**, *133*, 20130−20133.
(13) Lin, C. J.; Lee, W. Y.; Lu, C.; Lin, H. W.; Chen, W. C. *Macromolecules* **2011**, *44*, 9565−9573.
(14) Jing, J. M.; Yang, P. A.; Hsieh, T. S.; Wei, K. H. *Macromolecules* **2011**, *44*, 9155−9163.
(15) Bijleveld, J. C.; Zoombelt, A. P.; Mathijssen, S. G. J.; Wienk, M. M.; Turbiez, M.; Leeuw, D. M.; Janssen, R. A. J. *J. Am. Chem. Soc.* **2009**, *131*, 16616−166617.
(16) Zhang, Y.; Zou, J.; Yip, H. L.; Chen, K. S.; Zeigler, D. F.; Sun, Y.; Jen, A. K. Y. *Chem. Mater.* **2011**, *23*, 2289−2291.
(17) Schroeder, B. C.; Nielsen, C. B.; Kim, Y. J.; Smith, J.; Watkins, S. E.; Song, K.; Anthopoulos, T. D.; McCulloch, I. *Chem. Mater.* **2011**, *23*, 4025−4031.
(18) Nielsen, C. B.; Schroeder, B. C.; Hadipour, A.; Rand, B. P.; Watkins, S. E.; McCulloch, I. *J. Mater. Chem.* **2011**, *21*, 17642−17645.
(19) Feyter, S. D.; Gesquiere, A.; Schryver, F. C. *Chem. Mater.* **2002**, *14*, 989−997.
(20) Yang, X.; Wang, J.; Zhang, X.; Wang, Z.; Wang, Z. *Langmuir* **2007**, *23*, 1287−1291.
(21) Liu, J.; Gao, B. X.; Cheng, Y. X.; Xie, Z. Y.; Geng, Y. H.; Wang, L. X.; Jing, X. B.; Wang, F. S. *Macromolecules* **2008**, *41*, 1162−1167.
(22) Chen, J. J. A.; Chen, T. L.; Kim, B. S.; Poulsen, D. A.; Mynar, J. L.; Fréchet, J. M. J.; Ma, Biwu *ACS Appl. Mater. Interface* **2010**, *2*, 2679−2686.
(23) Osaka, I.; Akita, M.; Koganezawa, T.; Takimiya, K. *Chem. Mater.* **2012**, *24*, 1235−1243.
(24) Song, H. J.; Lee, S. M.; Lee, J. Y.; Choi, B. H.; Moon, D. K. *Synth. Met.* **2011**, *161*, 2451−2459.
(25) Osaka, I.; Abe, T.; Shinamura, S.; Miyazaki, E.; Takimiya, K. *J. Am. Chem. Soc.* **2010**, *132*, 5000−5001.
(26) Qin, R.; Li, W.; Li, C.; Du, C.; Veit, C.; Schleiermacher, H. F.; Andersson, M.; Bo, Z.; Liu, Z.; Ingana, O.; Wuerfel, U.; Zhang, F. *J. Am. Chem. Soc.* **2009**, *131*, 14612−14613.
(27) Lu, G.; Usta, H.; Risko, C.; Wang, L.; Facchetti, A.; Ratner, M. A.; Marks, T. J. *J. Am. Chem. Soc.* **2008**, *130*, 7670−7685.
(28) Blouin, N.; Michaud, A.; Gendron, D.; Wakim, S.; Blair, E.; Neagu-Plesu, R.; Belletete, M.; Durocher, G.; Tao, Y.; Leclerc, M. *J. Am. Chem. Soc.* **2008**, *130*, 732−742.
(29) Hou, J.; Chen, T. L.; Zhang, S.; Huo, L.; Sista, S.; Yang, Y. *Macromolecules* **2009**, *42*, 9217−9219.
(30) Gadisa, Abay.; Mammo, W.; L. Mattias Andersson, Admassie, S.; Zhang, F.; Andersson, M. R.; Inganäs, O. *Adv. Funct. Mater.* **2007**, *17*, 3836−3842.
(31) Kim, B. G.; Kim, M. S.; Kim, J. S. *ACS Nano* **2010**, *4*, 2160−2166.
(32) Wang, E.; Hou, L.; Wang, Z.; Ma, Z.; Hellstrom, S.; Zhuang, W.; Zhang, F.; Inganas, O.; Andersson, M. R. *Macromolecules* **2011**, *44*, 2067−2073.